Single molecule unfolding and stretching of protein domains inside a solid-state nanopore by electric field

Kevin J. Freedman, S. Raza Haq, Joshua B. Edel, Per Jemth, Min Jun Kim

Supplementary Information

TABLE OF CONTENTS

I. Nanopore experimental methods and characterization

Nanopores were drilled in a 50 nm thick free-standing silicon nitride membrane which was supported on all sides by a silicon chip (5.5×5.5 mm^2). Fabrication of this membrane consisted of first depositing a layer of low-stress silicon nitride on a silicon wafer using low pressure chemical vapor deposition (LPCVD) followed by photolithography, deep reactive ion etching (DRIE) and KOH etching to form a 50×50 μm^2 square membrane. Pores were then drilled using a focused electron beam (TEM JEOL 2010F FEG). Pore characterization and event recording was accomplished by placing the nanopore between two electrolytic half cells filled with buffered potassium chloride (2 M, 10 mM potassium phosphate buffer pH 7). The nanopore chip was held in place using a custom built polycarbonate flow cell with PDMS gaskets to assure that the only path of ionic current is through the nanopore. Electrodes (Ag/AgCl) were placed in both chambers and connected to the headstage of a patch clamp amplifier (Axopatch 200B, Molecular Devices Inc.) which allowed the ionic current to be measured at various applied voltages. Conductance measurements were conducted prior to each experiment and were found to be within 5% of each other. A TEM image of a 15 nm pore, along with current-voltage characteristics, is shown in Figure S1. Based on the IV curves, pore sizes had a deviation of no more than ±1-2 nm.

Prior to each experiment, protein solutions were made fresh by diluting the desired protein into buffered 1M KCl for a final protein concentration of 10 nM. After characterization of the pore, protein was injected into one chamber of the flow cell while a constant voltage is applied across the pore. Protein translocation events, defined as transient decreases in current, were detected using a threshold and characterizing features were extracted including event duration, event amplitude, and event area (integrated area of the entire event). Example ionic current recordings for the wild type SAP97 PDZ2 domain at different applied voltages are shown in Figure S2.

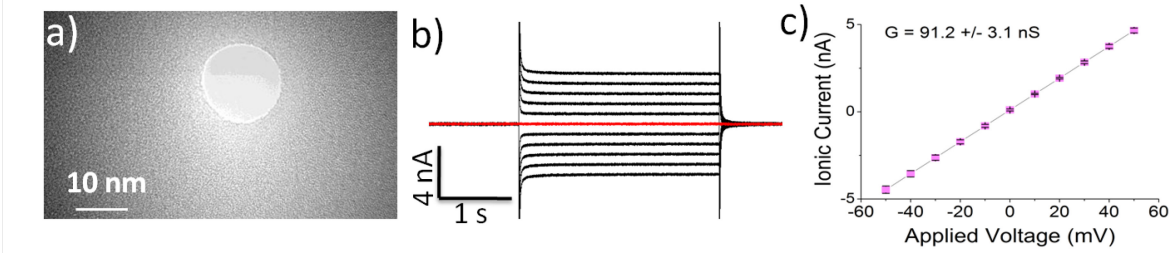

Fig. S1. Nanopore setup and electrical characterization of pores. (a) TEM image of a 15 nm pore drilled using a focused electron beam. Membrane thickness is 50 nm. (b) Ionic current recordings for step increases in voltage (-50 to 50 mV). (c) Mean current-voltage response for three 15 nm pores showing an ohmic response with an average pore conductance of 91.2 nS.

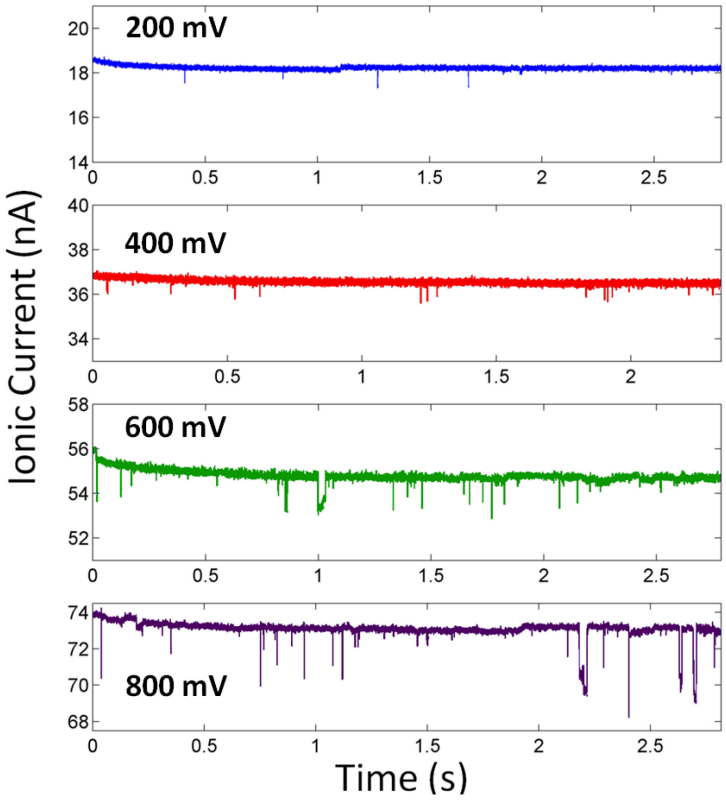

Fig. S2. Example ionic current measurements for four different applied voltages (200, 300, 600, 800 mV) for the SAP97 PDZ2 domain. Current drop and the frequency of events are observed to increase with voltage, as expected.

II. Protein preparations and stability analysis

Protein expression, purification and equilibrium denaturation

SAP97 PDZ2 was expressed and purified as described [1-2]. The mutants, L322A and V388A, were made by inverted PCR using the cDNA of SAP97 PDZ2 as a template. The purity of the proteins was checked by SDS-PAGE and their identity by mass spectrometry. Purified SAP97 PDZ2 variants were subjected to urea-induced unfolding experiments. The unfolding transition was monitored using Trp fluorescence (excitation at 280 nm and emission at 340 nm) and plotted as a function of urea concentration (Fig. S3). Data were analyzed using the general equation for solvent denaturation as described [1-2] to obtain the parameters $m_{D\text{-}N}$ (shared in the curve fitting) and $[\text{urea}]_{50\%}$, which were used to calculate $\Delta G_{D\text{-}N}$ and $\Delta\Delta G_{D\text{-}N}$.

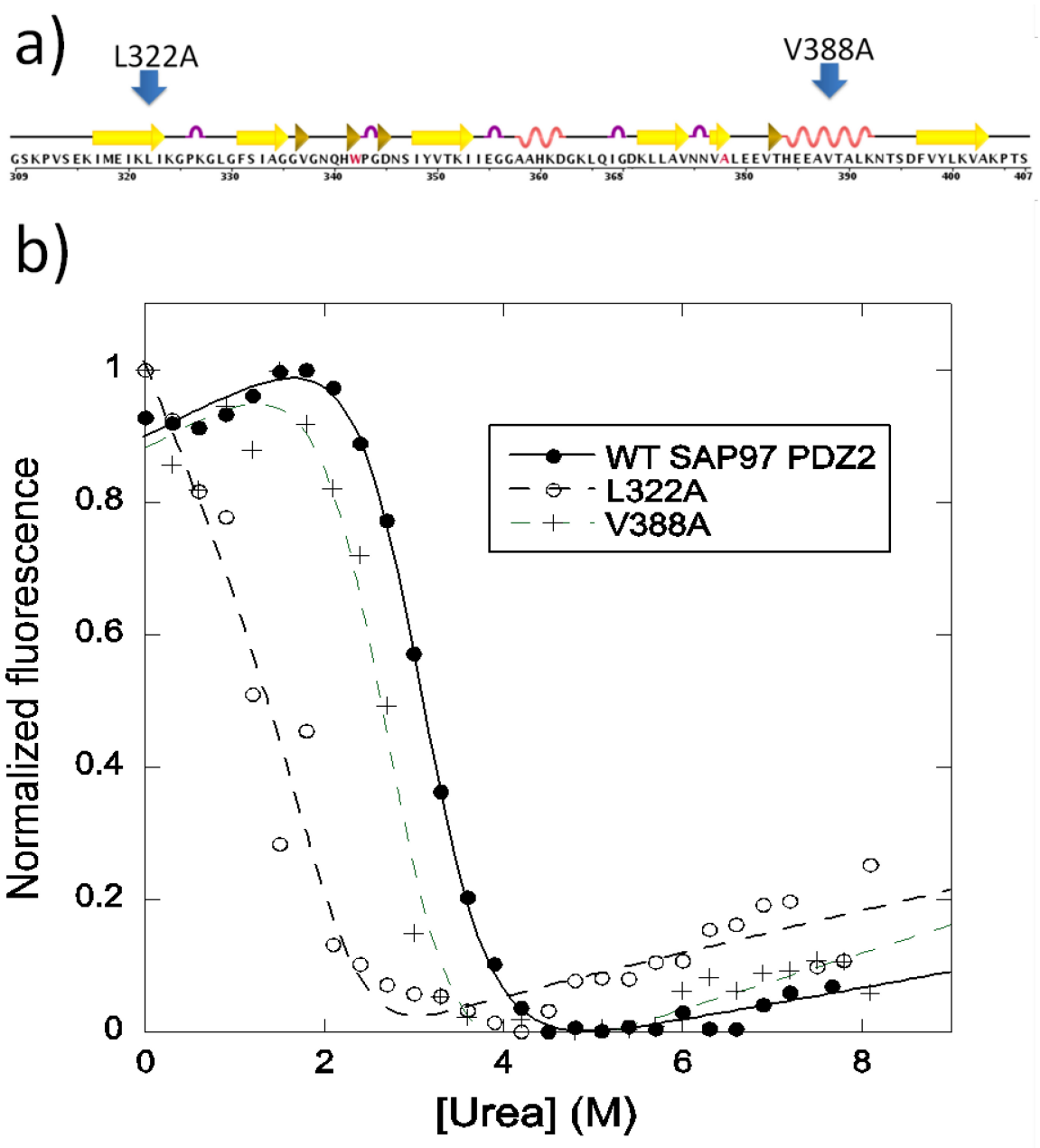

Fig. S3. (a) Wild type SAP97 PDZ2 (I342W/C378A) amino acid sequence with secondary structure graphically represented above the sequence. Arrows show where the two destabilizing mutations are located within the protein. (b) Equilibrium denaturation curves for each PDZ2 domain were obtined by measuring fluorescence as a function of urea concentration. Data were fitted assuming solvent denaturation of a two state system.

III. Finite element analysis

Simulating shape changes within a nanopore

One motivation for this work has been to develop methods to quantify stability; in particular using the electric field as a controllable way to denature proteins. In order to characterize the denatured states and understand the observed trends in excluded volume as a function of voltage, we considered an axial symmetric particle of radius r_p and length l_p submerged in an electrolyte solution fixed within the confines of a nanopore. The electrolyte is confined in a spherical vessel that is partitioned into two chambers by an insulating membrane of uniform surface charge ($-0.02\ Cm^{-2}$) [3]. The system was solved using coupled Nernst-Planck equations for the ion concentration fields (potassium and chloride) along with Stokes equations for the flow field [4]. In order to understand shape changes within a nanopore, simulations were run using several model shapes which evolved over the course of several simulations depending on the applied voltage. The types of shape transformations that were tested included both two-state protein folding models as well as gradual elongation models; each shape having a constant area inside the pore which blocked the flow of ions. We also investigated static particles over the same range of voltages; specifically for a fixed shape circular occluding particle and a fixed shape rod-shaped particle (Figure S4).

A fixed shape particle (both circular and rod-shaped) produced a linear increase current with increasing voltage (Fig. S5a). This is in contrast to what we observed experimental in which the current drop was best fit using a polynomial function. The linearity of both the current drop parameter and the baseline current as a function of voltage led to a constant value for the percentage of blocked current (Fig. S5b). If we then allow the particle to change shape at some defined voltage (in this case between the voltage 400 and 600 mV), we observe a decrease in percent blockage as the particle deforms from a circular particle to a rod-shaped particle with constant occluding area within the pore (Fig. S5b). This two state model did not explain the observed trends we saw experimentally and inevitably led to a two

state excluded volume curve. However, using a particle with an occluding area of 36 nm^2 that grew in length from 6 nm (roughly the long axis of a fully folded SAP97 PDZ2 molecule) to 36 nm (roughly the length of the fully linear SAP97 PDZ2 molecule), the observed trend agrees with the experimentally observed changes in excluded volume (Fig. S5c). Given the two dimensional nature of the simulation, we used the current blockade divided by the baseline current to obtain a measure directly relatable to the excluded volume. Both measures take into account the electrolyte conductivity and the increasing baseline current due to voltage increases.

Using a constant applied voltage (400 mV), changes in the current drop parameter were explicitly quantified and correlated to the shape of the translocating particle (Fig. S5d). The results show a drastic initial decrease in the current drop parameter followed by a comparatively minor increase followed by a leveling off. The region of the plot where current drop falls most dramatically (i.e. left of the dotted line in Fig. S4) the width of the particle undergoes the greatest change (marked by the large slope of the solid red line). After a length of 12.5 nm, the current becomes increasingly blocked as the length continues to grow and enters into a new regime of the plot where the length is changing the most dramatically. The increase in current at 12.5 nm is expected to be caused by interplay of the increasing length of the molecule and greater surface area to volume ratio. However due to the finite thickness of the membrane, the length of the molecule can only increase so much before it begins to reach the entrance and exit of the pore where it has less influence on the current [5]. This effect was not observed experimentally since PDZ2 has a contour length smaller than the membrane thickness. From this work, we correlated the changes in excluded volume with the shape of the molecule and provided evidence for the possible occurrence of increasing excluded volume as a folded protein becomes progressively unfolded by a one dimensional stretching force. Therefore at a given voltage, we would expect to be sampling from populations of protein conformations that exist somewhere along this curve representing the gradual unfolding of a protein.

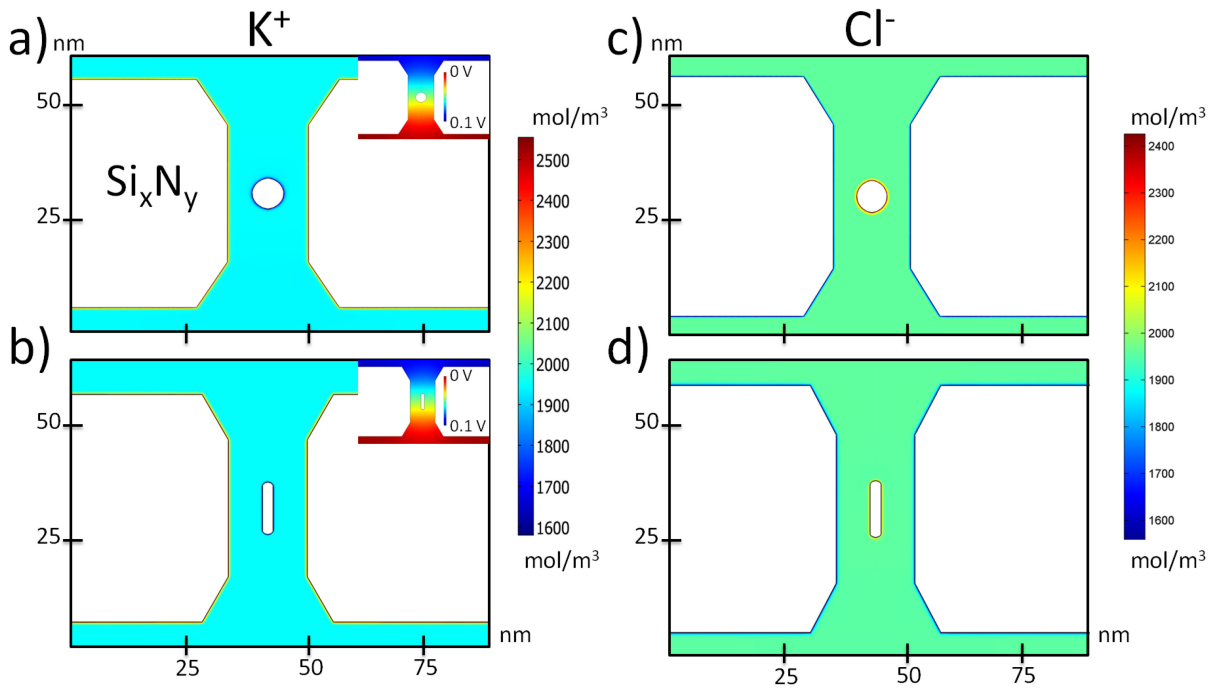

Fig. S4. Simulation geometries for circular and rod-shaped (length=10 nm) particles within a 15 nm pore (50 nm thick membrane) with an equal occluding area of 36 nm^2. (a-b) Ion distributions for the K^+ ion which shows an increased concentration at the nanopore wall due to the negative surface charge (-0.02 C m^{-2}) when compared to the bulk concentration (2 M KCl=2000 mol/m^3). The particle was assumed to have a surface charge of +0.016 C m^{-2} which results in a lower K+ concentration around the particle. Insets: Electric potential distributions for each geometry (in Volts). (c-d) Ion distributions for the Cl^- ion for the circular and rod-shaped geometries where the concentration around the particles is higher and the concentration at the pore is reduced compared to bulk.

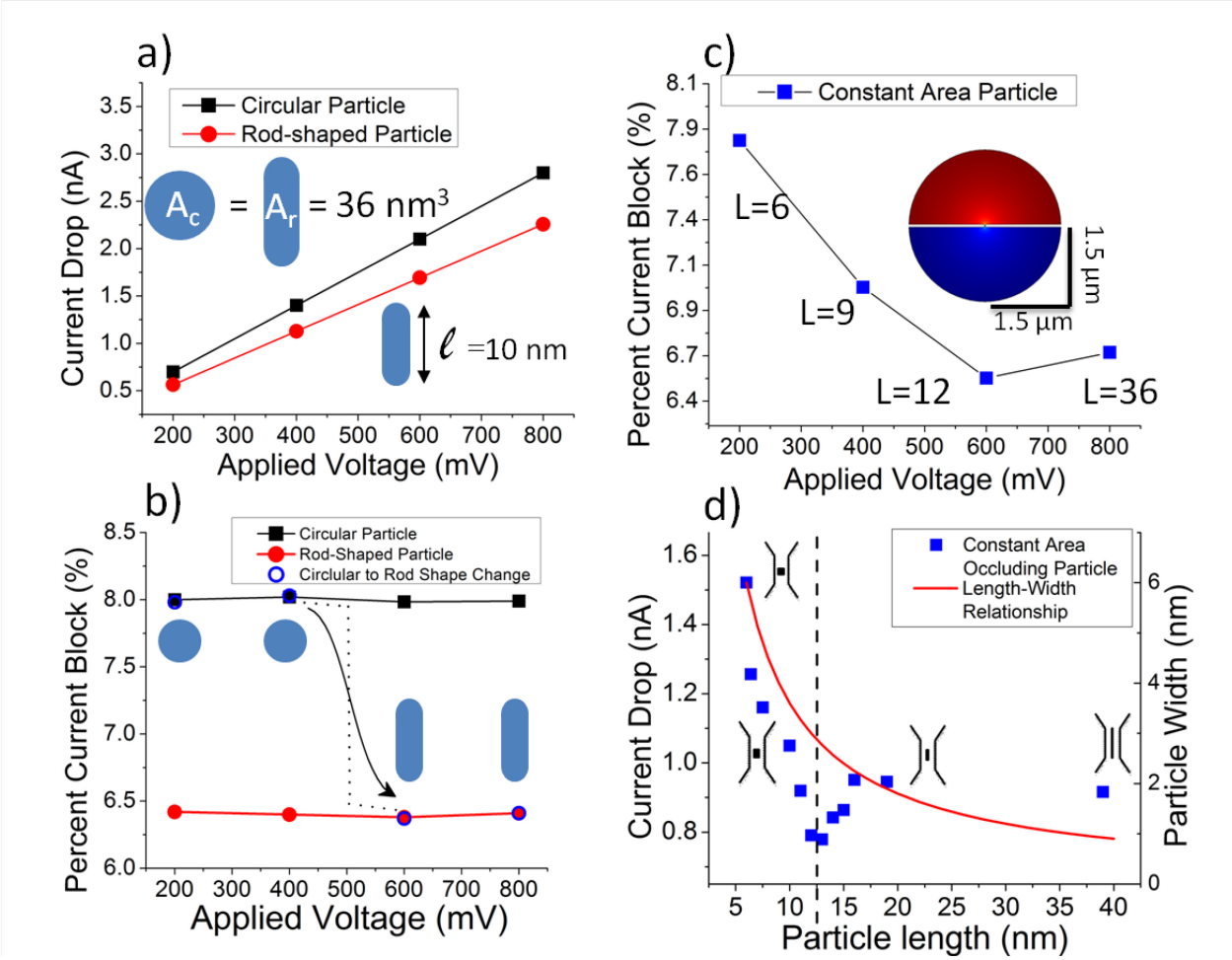

Fig. S5. Simulation results for a constant occluding area particle within a nanopore. (a) Current drop values for two equal area shapes across four different applied voltages. (b) Percent block (%) for a circular and rod-shaped occluding particle. (c) Percent block (%) dynamics for a particle undergoing a gradual elongation with a constant occluding area within the pore. Percent current block was calculated as the mean current reduction with the particle inside the pore divided by the open pore current. Inset: spherical electrolyte conduit separated by an insulating membrane. (d) Constant voltage (400 mV) simulations showing effect of a rod-shaped particle changing its aspect ratio while keeping a constant occluding area within the pore.

IV. Excluded volume calculations

Despite our initial speculation that the H_{eff} parameter in the excluded volume equation should be kept constant across voltages, several analyses were done to confirm this fact. As a first approximation, we calculated the half max full width of the electric field distribution obtained through numerical simulations (described above). The electric field distributions are shown in Fig. S6. We observed that although the electric field is naturally higher at the pore edges, the full width half max remains constant across voltages (approximately 65 nm as the theoretical length of the pore). As described in the main text, this however should not be used as the H_{eff} parameter in the excluded volume equation due to the inaccuracy of assuming the electric field is given by the applied voltage divided by the pore length. Using H_{eff} as a fitting parameter gets rid of this inaccuracy. Once H_{eff} is found using this method we believe the electric field contribution to the excluded volume equation is accounted for and given the electric field scales linearly with applied voltage, all other voltages would be accurately represented as well. This implies that the relative contributions of pore resistance (voltage drop within the pore) and access resistance (voltage drop just outside the pore) is not voltage dependent, as described previously.[6]

The fact that H_{eff} stays constant can also be indirectly confirmed by testing whether the current drop parameter is linear across a wide range of voltages for particles with fixes volumes. Since the linearity of the current drop parameter inevitably leads to a constant excluded volume across voltages (as it should), the way in which we calculate excluded volume can be confirmed to be accurate. Since most nanoparticles rapidly aggregate at the high salt conditions used here (2 M KCl), we could not experimentally confirm the linearity of the current drop parameter at our specific conditions. Instead we used numerical simulations of a spherical particle 5 nm in diameter (2 M KCl, +0.016 C m^{-2}). Since these simulations take into account access resistance (the voltage drop that occurs outside the pore), we can use these simulations to test whether the excluded volume equation is (1) accurate at a constant voltage and (2) accurate over a range of voltages using a constant H_{eff} value. The results (Fig. S7) indicated that the current drop is linear with applied voltage and, using a constant H_{eff} value, the excluded volume stays

constant. These results were also confirmed experimentally using 5 nm gold nanoparticles as shown in the main text. Event histograms for these data are shown in Fig. S9.

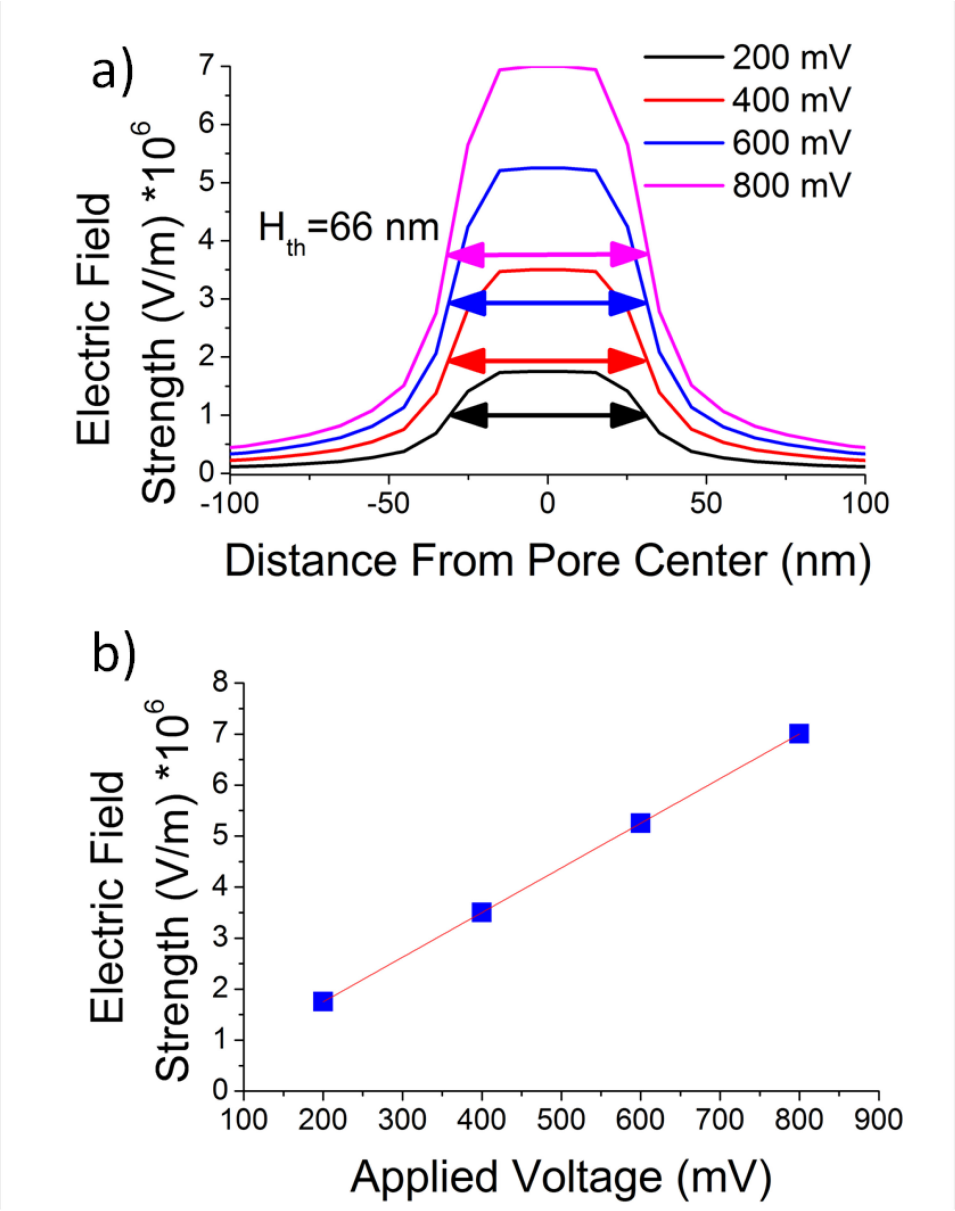

Fig. S6. Numerical simulations of the electric field inside and around the nanopore performed over a range of voltage (200-800 mV). (a) Electric field distribution along the axial direction of the nanopore plotted as the distance from the pore center (in nm). The colored arrows are all the same length and represent the full width half max of the distribution. (b) The linear increase in the strength of the electric field with applied voltage (in mV).

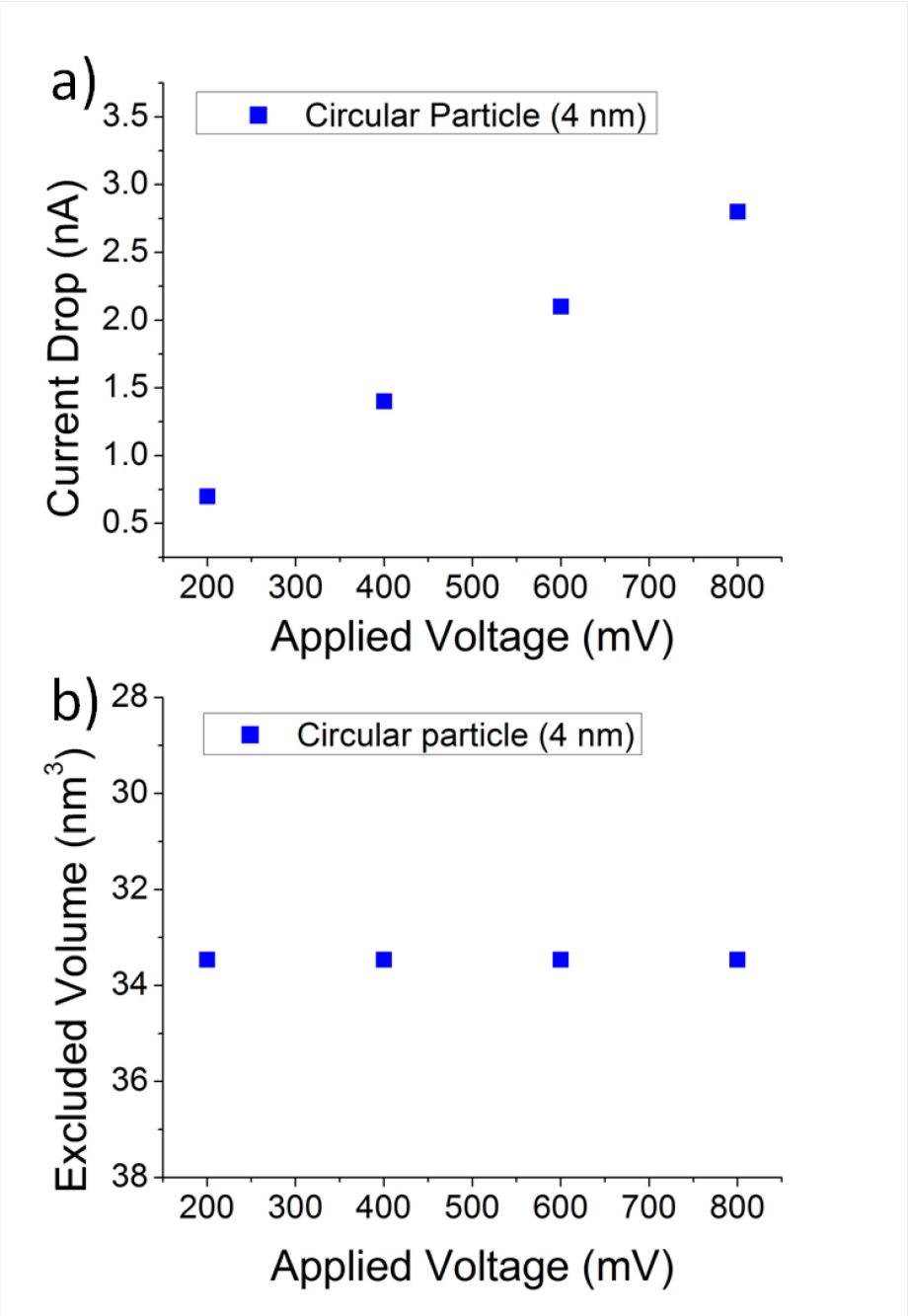

Fig. S7. Numerical simulations for the blocked flow of ions due to a 4 nm circular particle with a surface charge of +0.016 C m^{-2} over the range of 200-800 mV. (a) The current drop parameter plotted as a function of applied voltage showing a linear dependence. (b) The excluded volume parameter for a fixed

volume particle over the range of 200-800 mV. The H_{eff} value was used as a fitting parameter to the known volume (33.5 nm^3) and then kept constant across all voltages.

V. Translocation time histograms

Translocation times obtained in this work were well within the limits of detection as shown by previous works that characterized the minimum event durations that can be detected without filter attenuation [5,7]. In these works, it can be shown that 70 μs events are well within the range of detection using a 10 kHz filter. The shortest events obtained in this work were 77 μs. Also, when taking a close look at the event signature, the maximum current drop is not a singular point but rather stays blocked for several points. Furthermore, since the translocation time histograms (Fig. S8) generally led to a peaked distribution which decayed on both sides of the distribution, we can be fairly certain that the peak value is not an artifact of the low-pass filter used during recording.

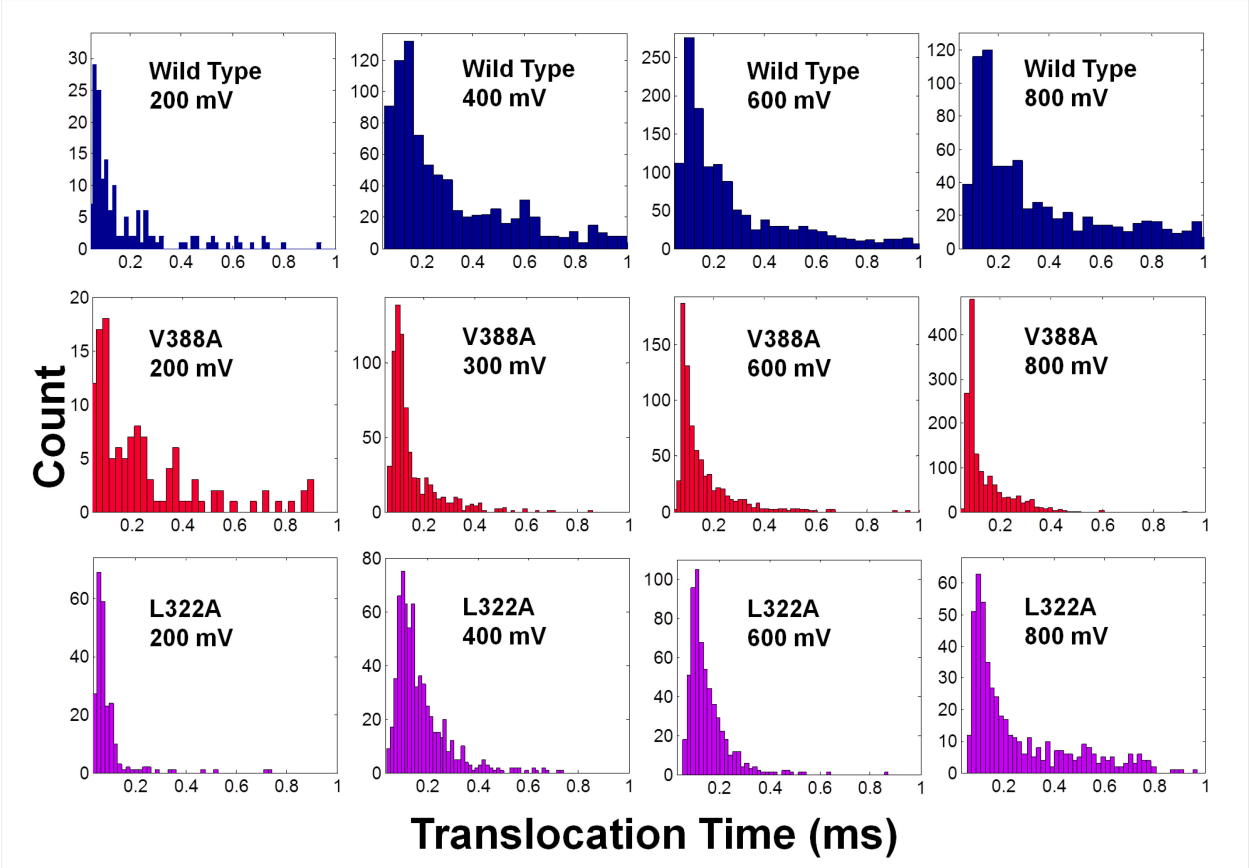

Fig. S8. Translocation time (i.e. residence time) for the wild type, V388A mutant, and L322A mutant PDZ2 domains at the specified applied voltage. Experimets were conducted at pH7 in 2 M KCl.

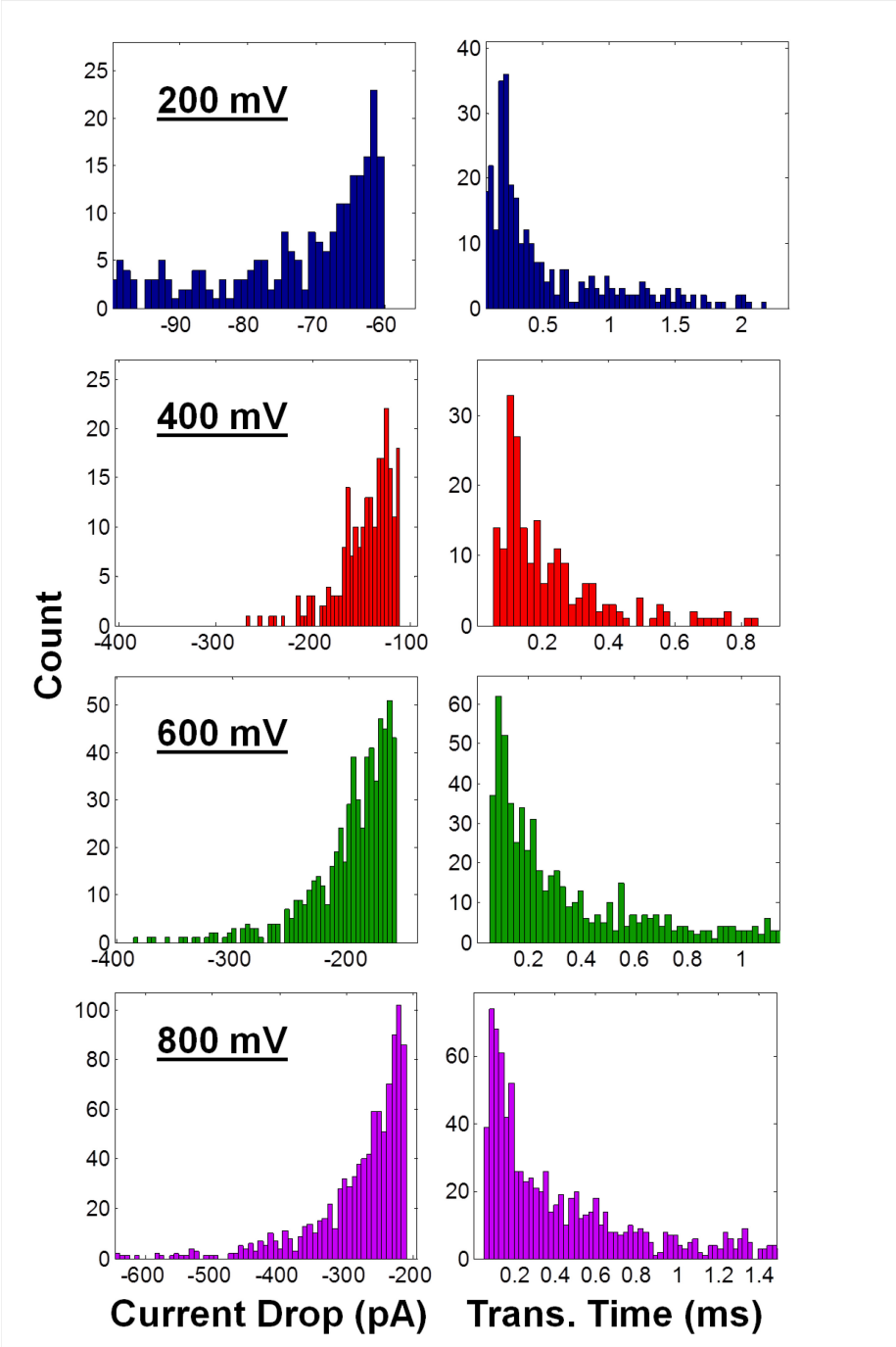

Fig. S9. Current drop and translocation time (i.e. residence time) histograms for 5 nm gold nanoparticles. Events were recorded at 200 (n=307), 400 (n=228), 600 (n=642), and 800 mV (n=981) in 0.2 M KCl (with 0.15 mM triton-100). The concentration of the gold nanoparticles (1 nM) as well as the concentration of KCl was kept low to reduce aggregation. All recordings were with a single 15 nm pore dilled using a TEM.

VI. REFERENCES

1. Chi, C. N. *et al.* A sequential binding mechanism in a PDZ domain. *Biochem.* **48**, 7089-7097 (2009).
2. Haq, S. R. *et al.* The plastic energy landscape of protein folding. *J. Biol. Chem.* **285**, 18051-18059 (2010).
3. Prabhu, A. S. *et al.* Chemically modified solid state nanopores for high throughput nanoparticle separation. *J. Phys. Condens. Matter* **22**, 454107 (2010).
4. Liu, H., Qian, S. & Bau, H. H. The effect of translocating cylindrical particles on the ionic current through a nanopore. *Biophys. J.* **92**, 1164-1177 (2007).
5. Talaga, D. S. & Li, J. Single-molecule protein unfolding in solid state nanopores. *J. Am. Chem. Soc.* **131**, 9287-9297 (2009).
6. Hille, B. *Ionic channels of excitable membranes*. 3 edn, p352 (Sinauer Associates Sunderland, MA, 1984).
7. Pedone, D., Firnkes, M. & Rant, U. Data analysis of translocation events in nanopore experiments. *Anal. Chem.* **81**, 9689-9694 (2009).